

Mathematical Modeling and Dynamical Aspects of the Co-Infection of Buruli Ulcer and Cholera

Asaf Khan

Department of Mathematics and Statistics,
University of Swat, Pakistan.

Email (Corresponding Author): asafkhan@uswat.edu.pk

Gauhar Ali

Department of Mathematics and Statistics,
University of Swat, Pakistan.

Email: mrgauhrali@gmail.com

Abdul Khaliq

Department of Mathematics and Statistics,
University of Swat, Pakistan.

Email: abdulkhaliq.edu.pk@gmail.com

Gul Zaman

Department of Mathematics,
University of Malakand, Pakistan.

Email: talash74@yahoo.com

Received: 02 February, 2024 / Accepted: 08 February, 2025 / Published online: 25 March, 2025

Abstract. The investigation and modelling of the co-infection of Buruli ulcer and Cholera are examined in this paper. We develop the model based on the current literature on the co-infection of these illnesses. The paper starts by discussing the submodels at the equilibrium points and outlining the mathematical characteristics of the solution. The underlying conditions are obtained, and the local and global stabilities of the fixed points of the sub-models are inspected. When R_0 is less than one, it is demonstrated that the sub-models are both globally and locally stable, demonstrating the stability of the state in the absence of infection. In addition, the co-infection model is analyzed concerning the parameter R_0 , and the co-infection model's disease-free state is locally stable under the stated condition. We also investigate the control problem with five distinct control variables. Pontryagin's maximal principle provides precise mathematical conclusions about the optimality system. This also helps find the best way to keep both diseases from spreading. We lastly conducted numerical

tests with different sets of parameter values, and the obtained analytical results are verified via simulations. The study's findings suggest that the best strategy to reduce infections is to put all preventative measures into place at once.

AMS (MOS) Subject Classification Codes: 93D05; 34C60; 37M05

Key Words: Epidemic models; Stability theory; Simulation; Lyapunov function.

1. INTRODUCTION

Any medical condition brought on by pathogens, including bacteria, viruses, fungi, parasites, or aberrant proteins called prions, is referred to as an infectious disease. People have had to face the difficulties these illnesses provide throughout history. There is a greater chance of illnesses spreading quickly and turning into epidemics as societies become more linked. As a result, illnesses including influenza, dengue fever, chickenpox, and tuberculosis (TB) have increased.

It has been shown that malaria is one of the deadliest illnesses; ancient accounts date its origin to 2700 BC in China [8]. An unidentified infectious agent caused the Plague of Athens, which is acknowledged as the first pandemic ever documented. When they fled the Spartan army in 430 B.C., around one-third of the populace perished from this virus [18]. More recently, leprosy created major problems in Europe in the eleventh century, and the deadly Black Death shocked the globe in the fourteenth century with its infectious illness outbreaks. Thirty to sixty percent of the European population perished as a result of the Black Death. The Russian Flu, which struck between 1889 and 1890, killed over 360,000 people worldwide, more than the World War I influenza epidemic. By the end of 1918, over 25 million people had died from a severe strain of Spanish influenza [37]. The human immunodeficiency virus (HIV) caused the AIDS pandemic, which was first recognized in 1981 as the 20th century's final significant pandemic. More than 32 million people have died from HIV/AIDS during the previous 40 years, and the disease is still considered a pandemic. WHO verified 574 deaths through laboratories among the 1,599 reported MERS-CoV cases in 2003 [20]. The SARS-associated coronavirus (SARS-CoV) virus is the cause of the illness. SARS-CoV most likely started in animals before spreading to people, according to health professionals; however, the exact source is still being looked into. The first pandemic of the twenty-first century was attributed to swine influenza and was proclaimed by the World Health Organization (WHO) in 2009 [40]. In December 2019, Wuhan, China, first identified COVID-19, a novel coronavirus disease that affects humans. Since the 1918 influenza pandemic, this was the sixth significant epidemic. The virus quickly spread to other regions of the world, and by September 2021, COVID-19 was known to have caused over 200 million confirmed cases and over 4.6 million recorded fatalities.

An infectious disease not only causes illnesses and deaths but also generates significant economic consequences; for instance, the foot-and-mouth disease outbreak in the UK resulted in losses exceeding 3 billion [36]. Additionally, secondary effects such as bat deaths in North America caused annual losses in agriculture amounting to USD 3.7 billion [7]. There is a major long-term influence on the transmission of infectious diseases due to the

growing global market and greater international travel [17]. Diseases like the swine flu and the Zika virus are major health concerns in many developing nations. Mosquitoes carrying the Zika virus are the main vector of infection; there is currently little scientific knowledge of this virus and no effective therapy [44]. As of August 8, 2022, there have been three fatalities from 20 recorded cases of leptospirosis in the Lindi area of the United Republic of Tanzania. Devastating effects of the Ebola virus have been seen in West Africa, where it has caused hemorrhagic fever, a severe condition known as Ebola viral sickness. Since it was discovered in 1976, millions of people have died from this virus, and its consequences are still felt today [43]. Since 2017, there has been a persistent outbreak of cholera in Somalia. There were 7,796 cases of cholera reported between January 1 and July 10, 2022; tragically, 37 of those cases resulted in death (case fatality ratio: 0.5%).

Mathematical modeling reduces real-world problems to straightforward formulae [34]. When used in the context of infectious illnesses, it helps with comprehension, epidemic prediction, and the creation of control plans. Acquiring and mastering this multidisciplinary ability is essential for resolving a wide range of issues [10]. Using a combination of methods, epidemic modeling, examines the spread and behavior of infectious diseases [5]. The severity of epidemics drives mathematicians and other researchers to work on managing and comprehending the dynamics of infectious diseases. The earliest formal mathematical analysis of epidemics dates back to Bernoulli's groundbreaking work on measles in the mid-1800s [6]; this work was later recast using differential equations [9]. Louis Pasteur made significant advances in the mid-1800s about the causes and prevention of illness. William Hamer's work at the beginning of the 20th century greatly advanced mathematical modeling, and Sir Ronald Ross is recognized as the founder of contemporary mathematical epidemiology. The first age-structured linear epidemic model was created by Kermack and McKendrick [16]. During the HIV epidemics of the 1980s, mathematical modeling of infectious illnesses gained popularity, resulting in the creation, evaluation, and use of several models to investigate the transmission of disease. These days, mathematical epidemiology is widely discussed in research publications, and modeling makes a major contribution to both public health and mathematics ([14, 19, 21, 35]).

To comprehend the transmission of infectious diseases within populations, epidemic models are indispensable instruments [16, 28]. The practicality of these models is significantly influenced by the degree of realism that is implemented into their design. This does not suggest that a single model should encompass every potential effect; rather, it should concentrate on simplifying the representation of the main mechanisms while preserving the major factors that affect disease transmission. Nonetheless, caution must be exercised when employing epidemic models to forecast real-world phenomena [33, 22]. The SIR model is a conventional compartmental framework commonly employed to elucidate several facets of epidemiological diseases [14, 27]; it is especially adept at representing the dynamics of illnesses such as measles, chickenpox, mumps, and rubella [4]. On the other hand, fractional calculus has become a powerful technique to model a wide range of epidemic diseases. It is more accurate than traditional methods at capturing complex dynamics of the infectious diseases. Standard mathematical models that use integer-order derivatives, even when the models are not linear, often have trouble explaining how many real-world epidemics behave in a way that makes sense. In recent years, fractional calculus has gotten a lot of attention as a more realistic way to model epidemics because it can include memory

effects and genetic properties (see, for example, [30]). This method has worked especially well for solving problems related to long-term disease dynamics and strange diffusion processes [24]. Besides fractional differential equations, researchers used stochastic and delay differential equations to better understand the hidden aspect of infectious disease using a realistic approach of modeling.

The 19th-century identification of cholera, an epidemic brought on by the *Vibrio cholera* bacteria, is attributed to John Snow. It is quite common in Africa, especially in Sub-Saharan areas; the earliest cases were reported from Guinea in West Africa [25]. Every year, cholera strikes 35 million people, mostly in Asian and African regions [42]. Tainted food and water supplies are the main sources of its spread. *Mycobacterium ulcerans*, the source of another well-known illness, Buruli ulcer (BU), is primarily found in tropical areas; over 80% of cases have been documented from West African countries, including Ghana, Benin, and Cameroon [15, 11, 2]. To treat a BU infection, it is important to find it early and treat it with antibiotics like streptomycin and rifampicin for at least eight weeks [41]. To optimize tactics for reducing the spread of cholera, control measures are integrated into a model [13] in [23]. Cholera and Buruli ulcer co-infection is common in Asia and Sub-Saharan Africa, particularly in Ghana, where artisanal mining causes cholera epidemics because of fixed water bodies and poor hygiene [26]. The goal of this study is to gain a thorough understanding of the co-infection of cholera and Buruli ulcers, a problem that has received less attention than other illnesses. A comprehensive understanding of both illnesses is necessary in developing nations, especially in West Africa and Asia; examining their dynamics together can provide additional insights into their co-infection. Zhao et al. [45] investigated the co-dynamics of Buruli ulcer and cholera, developing a SIR type of model, and the detailed mathematical analysis of the sub-models was rigorously investigated. While this work significantly contributes to the existing literature on the co-dynamics of infections, it fails to consider the latent stage associated with Buruli ulcer. The novelty of the present work is that it considers the latent stage of Buruli Ulcer and studies its co-dynamics with Cholera. Further, the proposed study focusing on formulating and studying the stability of a susceptible-exposed-infected-recovered (SEIR) epidemic model, and the application of different control strategies to minimize the spread of both infection within the population. We intend to include individuals that are exposed to BU in modeling as a separate compartment. This will change majority of the dynamics pertaining to the existing model as well as close to the reality. Further, we intend to extend the control problem and see the effect of latent compartment on the entire control program.

The rest of the manuscript is organized as follows. Section 2 presents the model formulation and stability analysis of the co-infected model. Subsequently, dynamics of the sub-models are explored using the respective basic reproduction numbers. In Section 4, control variables are considered, and an optimal control problem is formulated utilizing the Pontryagin maximum principle. Section 5 includes numerical simulations of the co-infection model, both with and without control problems, verifying analytical results and thoroughly investigating the effectiveness of the control measures. Finally, Section 6 concludes the work and suggests future research directions.

2. MODEL FORMULATION

In this section, we intend to formulate a mathematical model for the co-infection of Cholera and Buruli ulcer epidemics and will present the local and global stability results for the equilibria of the underlying sub-models. To formulate the model, we shall denote the total human population by N_h and it is divided further into susceptible humans S_h ; the people who have been expose to Buruli ulcer only is E_b ; the people who have been infected with Buruli ulcer only I_b ; the people infected with Cholera only I_c ; people infected with Cholera and Buruli ulcer both D_{bc} ; the people recovered only from Buruli ulcer R_b ; the people recovered from the Cholera infection R_c ; and the recovered individuals both from the the Cholera and Buruli ulcer is R_{bc} . Thus $N_h = S_h + I_b + I_c + D_{bc} + E_b + R_b + R_c + R_{bc}$. We use N_v to represent the population of vectors and will divide this population into infected water bugs and susceptible, respectively denoted by S_v and I_v , with $N_v = S_v + I_v$. The probability of getting infected with cholera is denoted by β_1 , where $\beta_1 = \frac{zB}{\kappa+B}$, here B denotes the bacteria density, the rate of ingestion is z .

Other parameters of the model along with the descriptions are outlined in Table 1.

TABLE 1. Parameters and its interpretations.

Parameter	Description
π_h	The rate of recruitment of the healthy individuals.
π_v	The recruitment rate of water bugs.
ϕ	Caution regarding immunity and recovery rates in individuals infected with Buruli ulcer.
ψ	Caution about immunity and recovery rates in individuals affected by cholera.
θ	Advisory on the immunity status among co-affected individuals.
μ_h	Natural death rate in humans
μ_b	the death rate of Bacteria
β_h	the Buruli ulcer transmission probability.
β_v	TThe chances of water bugs becoming affected with Buruli ulcer
κ	the death related Buruli ulcer
ϖ	Among co-infected buruli ulcer related death .
ℓ	the death related Cholera .
ℓ	Among co-infected the Cholera death rate.
λ	the human contact rate with mycobacterium ulcerans.
ω	The contribution to the aquatic due to cholera infected
ρ	Modification of the parameter
η	The recuperation of individuals affected by Buruli ulcer.
σ	the affected individuals recovery of Cholera.
δ	the co-infected individuals recovery rate
ε	Individuals who exclusively recovered from co-infection with Buruli ulcer.
z	the Level of Ingestion
κ	In water the concentration of Mycobacterium ulcerans .

The following system of differential equations describes the dynamics of the coinfection of both BU and cholera:

$$\left\{ \begin{array}{l} \frac{dS_h}{dt} = \pi_h + \phi R_b + \Psi R_c + \theta R_{bc} - (\beta_h I_v + \beta_1) S_h - \mu_h S_h, \\ \frac{dE_b}{dt} = \beta_h I_v S_h - (\alpha + \mu_h) E_b - \beta_1 E_b, \\ \frac{dI_b}{dt} = \alpha E_b - \beta_1 I_b - (\eta + \mu_h + \kappa) I_b, \\ \frac{dI_c}{dt} = \beta_1 S_h - \beta_h I_v I_c - (\sigma + \mu_h + l) I_c, \\ \frac{dD_{bc}}{dt} = \beta_h I_v I_c + \beta_1 (I_b + E_b) - (\delta + \mu_h + \gamma + \varpi) D_{bc}, \\ \frac{dR_b}{dt} = \eta I_b - (\phi + \mu_h) R_b + \epsilon (1 - \delta) D_{bc}, \\ \frac{dR_c}{dt} = \sigma I_c - (\psi + \mu_h) R_c + (1 - \epsilon) (1 - \delta) D_{bc}, \\ \frac{dR_{bc}}{dt} = \delta D_{bc} - (\theta + \mu_h) R_{bc}, \\ \frac{dB}{dt} = \omega (I_c + \rho D_{bc}) - \mu_b B, \\ \frac{dS_v}{dt} = \pi_v - \beta_v (I_b + D_{bc}) S_v - \mu_v S_v, \\ \frac{dI_v}{dt} = \beta_v (I_b + D_{bc}) S_v - \mu_v I_v. \end{array} \right. \quad (2. 1)$$

In the subsequent section, we will present the well-posedness of the model.

2.1. Positivity and Boundedness of Solution. In order to guarantee that the solution with positive initial conditions remain positive for all $t \geq 0$, it is imperative to confirm that all state variables remain nonnegative for system (2. 1). The following theorem is established in a manner analogous to that of [31, 32]. Any solution $(S_h, E_b, I_b, I_c, D_{bc}, R_b, R_c, R_{bc}, B, S_v, I_v)$ of system (2. 1) remain positive for a set of positive initial conditions and all time $t \geq 0$.

Proof. To check the positivity of S_h , let us assume that all other state variables are non-negative for all time t . Further, let assume that $S_h(0) > 0$ and later on at time t_1 , it crosses t -axis for becoming negative, that is, $S(t_1) = 0$. However, by looking into the first equation of model (2. 1), we can write

$$\frac{dS_h}{dt} \Big|_{t=t_1} = \pi_h + \phi R_b + \Psi R_c + \theta R_{bc} \geq 0.$$

This shows that as soon the curve S_h reach t -axis, the curve is going back to the positive cone of the solution space and hence cannot be negative. To prove the positivity of E_b , we will follow a similar argument. Let $E_b(t_2) = 0$, then

$$\frac{dE_b}{dt} \Big|_{t=t_2} = \beta_h I_v S_h \geq 0.$$

Here again, the positivity of E_b is ensured. It is very simple to show the positivity of the remaining variables and hence we omitted its proof. All feasible solution of the system (

2. 1) are bounded and enter the region

$$\mathcal{Z} = \left\{ (S_h, E_b, I_b, I_c, D_{bc}, R_b, R_c, R_{bc}, B, S_v, I_v) \in R_+^{11} : N_h \leq \frac{\pi_h}{\mu_h} \wedge N_v \leq \frac{\pi_v}{\mu_v} \right\}.$$

Proof. By adding those equations of model (2. 1) which describe the dynamics of human population, we get the following equation

$$\frac{dN_h}{dt} = \pi_h - \mu_h N_h - (\delta + \gamma)D_{bc} - \omega I_c.$$

From the above relation, we can write

$$\frac{dN_h}{dt} \leq \pi_h - \mu_h N_h,$$

and by solving this differential inequality, we have $N_h(t) \leq \frac{\pi_h}{\mu_h}$. The boundedness of bacteria population B is trivial from the boundedness of I_c and D_{bc} . Likewise, by adding equations of model (2. 1) concerning vectors population, we have

$$\frac{dN_v}{dt} = \pi_v - \mu_v N_v,$$

which leads to $N_v(t) \leq \frac{\pi_v}{\mu_v}$ ensuring the boundedness of solution S_v and I_v and hence the result.

3. RESULTS ON THE DYNAMICAL ANALYSIS

We will provide a comprehensive examination of the whole model later on and initially, the sub-models will be investigated for stability purposes. Our analysis commences with the sub-model related to cholera. The sub-model for Cholera is derived by considering equations related to Cholera only and ignoring other relations. Thus, in the following subsection, we will consider the sub-model for Cholera.

3.1. Cholera sub-model. By considering the model' equations that govern the dynamics of the Cholera are given by the following submodel:

$$\begin{cases} \frac{dS_h}{dt} = \pi_h + \psi R_c - \beta_1 S_h - \mu_h S_h, \\ \frac{dI_c}{dt} = \beta_1 S_h - (\sigma + \mu_h + \ell) I_c, \\ \frac{dR_c}{dt} = \sigma I_c - (\psi + \mu_h) R_c, \\ \frac{dB}{dt} = \omega I_c - \mu_b B. \end{cases} \quad (3. 2)$$

Next, we will explore the mathematical characteristics and dynamical aspects of the cholera sub-model.

The disease-free equilibrium of the sub-model (3. 2) is given by the following equilibrium state:

$$E_{c0} = (S_h^*, I_c^*, R_c^*, B^*) = \left(\frac{\pi_h}{\mu_h}, 0, 0, 0 \right). \quad (3. 3)$$

The basic reproduction number for the sub-model (3. 2) is calculated as follows. Firstly, we have to consider the infected classes I_c and B from the sub-model (3. 2). Then we follows the standard procedure of next-generation matrix [38] and will form two matrix from these infected classes. One of these two matrices will contain linear and the other will assumes the non-linear terms as:

$$F = \begin{pmatrix} \frac{BzS_h}{\kappa+B} \\ 0 \end{pmatrix}, \quad V = \begin{pmatrix} \sigma + \mu_h + \ell I_c \\ -\omega I_c + \mu_b B \end{pmatrix},$$

in such a way that $\frac{dx}{dt} = F - V$ where $x = \begin{pmatrix} I_c(t) \\ B(t) \end{pmatrix}$. Next, we compute the Jacobian matrices for F and V as:

$$J(F) = \begin{pmatrix} 0 & \frac{(\kappa+B)(zS_h - BzS_h)}{(\kappa+B)^2} \\ 0 & 0 \end{pmatrix} \implies J(F) = \begin{pmatrix} 0 & \frac{\kappa z S_h + BzS_h - BzS_h(zS_h - BzS_h)}{(\kappa+B)^2} \\ 0 & 0 \end{pmatrix}.$$

Considering the disease-free equilibrium (DFE) given in relation (3. 3), we have the Jacobian matrices for F at the DFE as follows:

$$J(F) = \begin{pmatrix} 0 & \frac{z\pi_h}{\kappa\mu_h} \\ 0 & 0 \end{pmatrix},$$

because $S_h = \frac{\pi_h}{\mu_h}$ and $B = 0$.

Similarly, we calculate the Jacobian matrix for V st the DFE as:

$$J(V) = \begin{pmatrix} \sigma + \mu_h + \ell & 0 \\ -\omega & \mu_b \end{pmatrix}.$$

Let $A = J(F)$ and $B = J(V)$. Then, one can find the inverse of B , denoted as B^{-1} , as:

$$B^{-1} = \frac{1}{\mu_b(\sigma + \mu_h + \ell)} = \begin{pmatrix} \mu_b & 0 \\ \omega & \sigma + \mu_h + \ell \end{pmatrix}.$$

Next, we have to calculate the product AB^{-1} , that is:

$$AB^{-1} = \frac{1}{\mu_b X} \begin{pmatrix} \frac{z\pi_h\omega}{\kappa\mu_h} & \frac{z\pi_h\omega}{\kappa\mu_h} X \\ 0 & 0 \end{pmatrix},$$

where $X = (\sigma + \mu_h + \ell)$. To make the process simpler, we shall define $C = AB^{-1}$. The eigenvalues for C are found by solving the equation $\det(C - \lambda I) = 0$, that is:

$$\det \left(\begin{pmatrix} \frac{z\pi_h\omega}{\kappa\mu_b X} - \lambda & \frac{z\pi_h}{\kappa\mu_h\mu_b} \\ 0 & -\lambda \end{pmatrix} \right) = 0.$$

By solving the above relation for λ , we get

$$-\lambda \left(\frac{z\pi_h\omega}{\kappa\mu_b X} - \lambda \right) = 0,$$

or

$$\lambda = 0 \quad \text{or} \quad \lambda = \frac{z\pi_h\omega}{\kappa + \mu_h + \mu_b X}.$$

Thus, the basic reproduction number (R_{0_c}) for the Cholera sub-model is given by

$$R_{0_c} = \frac{z\pi_h\omega}{\kappa\mu_h\mu_b(\sigma + \mu_h + \ell)}.$$

In the subsequent theorem, we shall prove the local stability of the DFE for the Cholera sub-model (3.2). The DFE E_{c_0} of the Cholera sub-model (3.2) is locally asymptotically stable (LAS) if $R_{0_c} < 1$, and unstable for $R_{0_c} \geq 1$.

Proof. To prove the local asymptotic stability of the DFE E_{c_0} , we shall assume each class of sub-model (3.2) and will partially differentiate it with w.r.t S_h, I_c, R_c, B to find the Jacobean matrix as follows:

$$A = \begin{pmatrix} -\mu_h & 0 & \psi & -\frac{z\pi_h}{\kappa\mu_h} \\ 0 & -\ell - \sigma & 0 & \frac{z\pi_h}{\kappa\mu_h} \\ 0 & 0 & -\psi - \mu_h & 0 \\ 0 & \omega & 0 & -\mu_b \end{pmatrix}. \quad (3.5)$$

The characteristic equation for matrix A can be obtained as

$$\det(A - \lambda I) = 0.$$

By using matrix A and the identity matrix I , we have

$$\det \left(\begin{pmatrix} -\mu_h & 0 & \psi & -\frac{z\pi_h}{\kappa\mu_h} \\ 0 & -\ell - \sigma & 0 & \frac{z\pi_h}{\kappa\mu_h} \\ 0 & 0 & -\psi - \mu_h & 0 \\ 0 & \omega & 0 & -\mu_b \end{pmatrix} - \lambda \begin{pmatrix} 1 & 0 & 0 & 0 \\ 0 & 1 & 0 & 0 \\ 0 & 0 & 1 & 0 \\ 0 & 0 & 0 & 1 \end{pmatrix} \right) = 0.$$

Expanding the determinant, we have the following equation

$$(\lambda + \mu_h)((\lambda + \ell + \sigma + \mu_h)(\lambda + \mu_b)(\lambda + \psi + \mu_h) - \frac{z\pi_h}{\kappa\mu_h}(\omega\lambda + \omega\psi + \omega\mu_h)) = 0.$$

By simplification and rearranging the terms, we get

$$\begin{aligned} (\lambda + \mu_h)(\lambda + \psi + \mu_h)(\lambda^2 + \lambda\Phi_1 + \mu_b(\ell + \sigma + \mu_h)(1 - R_{0_c})) &= 0, \\ (\lambda + \mu_h)(\lambda + \psi + \mu_h)(\lambda^2 + \lambda\Phi_1 + \Phi_2) &= 0, \end{aligned} \quad (3.6)$$

where $\Phi_1 = \ell + \sigma + \mu_h + \mu_b$ and $\Phi_2 = \mu_b(\ell + \sigma + \mu_h)(1 - R_{0_c})$.

It can be seen from equation (3.6) that $\lambda_1 = -\mu_h$ and $\lambda_2 = -\psi - \mu_h$ are negative, while the quadratic equations $\lambda^2 + \lambda\Phi_1 + \Phi_2 = 0$ will give two other negative roots depends on R_{0_c} . It is clear from the definitions of Φ_i that the the coefficient $\Phi_1 > 0$ and $\Phi_2 > 0$ when $R_{0_c} < 1$. Therefore, according to Descartes rule of signs, if Φ_1 and Φ_2 are positive co-efficient of equation $\lambda^2 + \lambda\Phi_1 + \Phi_2 = 0$, then there does not exist any positive real root.

Now for negative real roots, we will replace λ by $-\lambda$ in the given equation as:

$$(-\lambda)^2 + \Phi_1(-\lambda) + \Phi_2 = 0 \implies \lambda^2 - \lambda\Phi_1 + \phi_2 = 0. \quad (3.7)$$

Here, we consider the sign alterations from positive to negative and again, by Descartes rules of signs, two negative real roots exist. In case of two negative roots, our theorem is proved as all of the four eigenvalues of the variational matrix are negative.

In case of zero negative real root of the underlying quadratic equation, roots are complex because complex are always in conjugate form. In this case, Descartes rule guaranteed that the real parts are negative. Hence, all of the eigenvalues are negative or complex with negative real parts. Thus, by following [39] (Theorem 3.3), the DFE of sub-model (3.2)

) is locally asymptotically stable under the condition of $R_{0c} < 1$. If $R_{0c} < 1$ and $\Psi = 0$, then the DFE E_{0c} of the cholera-only model is globally asymptotically stable.

Proof. To prove the theorem, we will define the Lyapunov function in the following form:

$$L(t) = m_1(1 - S_h^* - S_h^* \log \frac{S_h}{S_h^*}) + m_2 I_c + m_3 B. \quad (3. 8)$$

In the function $L(t)$, m_i for $i = 1, 2, 3$ represent constant that will be chosen later. Differentiate the function $L(t)$ w.r.t time, we get

$$\begin{aligned} \frac{dL(t)}{dt} &= m_1(1 - \frac{S_h^*}{S_h}) \frac{dS_h}{dt} + m_2 \frac{dI_c}{dt} + m_3 \frac{dB}{dt}, \\ &= \frac{m_1}{S_h} (S_h - S_h^*) (\mu_h S_h^* + \Psi R_c - \beta_1 S_h - \mu_h S_h) + m_2 (\beta_1 S_h - X_1 I_c) + m_3 (\omega I_c - \mu_b B), \\ &= -\frac{m_1}{S_h} (S_h - S_h^*)^2 \mu_h + \frac{m_1}{S_h} (S_h - S_h^*) (\psi R_c - \beta_1 S_h) + m_2 (\beta_1 S_h - X_1 I_c) \\ &\quad + m_3 (\omega I_c - \mu_b B), \\ &= -m_1 \frac{\mu_h}{S_h} (S_h - S_h^*)^2 + m_1 \psi R_c - m_1 \beta_1 S_h - \frac{m_1}{S_h} S_h^* \psi R_c + m_1 S_h^* \beta_1 + m_2 \beta_1 S_h \\ &\quad - m_2 X_1 I_c + m_3 \omega I_c - m_3 \mu_b B. \end{aligned}$$

Since we assumed that $\psi = 0$, so the above relation becomes:

$$\frac{dL(t)}{dt} = -m_1 \frac{\mu_h}{S_h} (S_h - S_h^*)^2 - m_1 \beta_1 S_h + m_1 S_h^* \beta_1 + m_2 \beta_1 S_h - m_2 X_1 I_c + m_3 \omega I_c - m_3 \mu_b B.$$

By choosing the constants $m_1 = m_2$, the above relation becomes:

$$\frac{dL(t)}{dt} = -m_1 \frac{\mu_h}{S_h} (S_h - S_h^*)^2 + m_1 S_h^* \beta_1 - m_2 X_1 I_c + m_3 \omega I_c - m_3 \mu_b B. \quad (3. 9)$$

Next, we set $m_3 \omega = m_2 X_1$ and considering the relation

$$-m_2 X_1 I_c + m_3 \omega I_c = m_2 (\sigma + \mu_h + \ell) \left(\frac{m_3 \omega}{m_2 (\sigma + \mu_h + \ell)} - 1 \right) I_c, \quad (3. 10)$$

and by assuming

$$\frac{m_3}{m_2} = \frac{\pi_h z}{\kappa \mu_b \mu_h}, \quad (3. 11)$$

relation (3. 10) becomes

$$\begin{aligned} -m_2 X_1 I_c + m_3 \omega I_c &= m_2 (\sigma + \mu_h + \ell) \left(\frac{m_3 \pi_h z \omega}{m_2 ((\kappa \mu_b \mu_h) \sigma + \mu_h + \ell)} - 1 \right) I_c, \\ &= m_2 (\sigma + \mu_h + \ell) (R_0 - 1) I_c. \end{aligned} \quad (3. 12)$$

By putting the above relation in place of terms on the left in relation (3. 9), we get

$$\frac{dL(t)}{dt} = -m_1 \frac{\mu_h}{S_h} (S_h - S_h^*)^2 + m_1 S_h^* \beta_1 + m_2 (\sigma + \mu_h + \ell) (R_0 - 1) I_c - m_3 \mu_b B. \quad (3. 13)$$

Now, keeping in mind the value of β_1 and considering the terms $m_1 S_h^* \beta_1 - m_3 \mu_b B$ as

$$\begin{aligned} m_1 S_h^* \frac{zB}{\kappa + B} - m_3 \mu_b B &= \frac{1}{\kappa + B} (m_1 S_h^* zB - m_3 \mu_b B(\kappa + B)), \\ &= \frac{B}{\kappa + B} (m_1 S_h^* z - m_3 \mu_b \kappa) - \frac{B}{\kappa + B} m_3 \mu_b B. \end{aligned}$$

In the above relation, the terms $\frac{B}{\kappa + B} (m_1 S_h^* z - m_3 \mu_b \kappa) = 0$ by using (3. 11) and $m_1 = m_2$. Thus, we can write

$$m_1 S_h^* \frac{zB}{\kappa + B} - m_3 \mu_b B = -\frac{B}{\kappa + B} m_3 \mu_b B. \quad (3. 14)$$

We can write (3. 13) if we use relation (3. 14) as

$$\frac{dL(t)}{dt} = -m_1 \frac{\mu_h}{S_h} (S_h - S_h^*)^2 + m_2 (\sigma + \mu_h + \ell) (R_{0_c} - 1) I_c - \frac{B}{\kappa + B} m_3 \mu_b B. \quad (3. 15)$$

Clearly, the right hand side of (3. 15) is negative only if $R_{0_c} < 1$ and hence by the LiapunovLasalle theorem [12] (p. 296), we can say that the DFE is globally asymptotically stable only if $R_{0_c} < 1$ and $\Psi = 0$, and unstable otherwise and hence the theorem.

3.2. The BU sub-model. To analyze the dynamics of BU, we will consider the model equations that govern the dynamics of the Buruli ulcer which are given by the following sub-model;

$$\left\{ \begin{aligned} \frac{dS_h}{dt} &= \pi_h + \phi R_b + -\beta_h I_v S_h - \mu_h S_h, \\ \frac{dE_b}{dt} &= \beta_h I_v S_h - (\alpha + \mu_h) E_b - \beta_1 E_b, \\ \frac{dI_b}{dt} &= \alpha E_b - (\eta + \mu + \kappa) I_b, \\ \frac{dR_b}{dt} &= \eta I_b - (\phi + \mu_h) R_b, \\ \frac{dS_v}{dt} &= \pi_v - \beta_v I_b S_v - \mu_v S_v, \\ \frac{dI_v}{dt} &= \beta_v I_b S_v - \mu_v I_v, \end{aligned} \right. \quad (3. 16)$$

Next, we will explore the mathematical characterizations and dynamical aspects of the Buruli ulcer sub model.

The disease-free equilibrium for the Buruli ulcer sub-model (3. 16) is given by the following relation

$$E_{b_0} = (S_h^*, E_b^*, I_b^*, R_b^*, S_v^*, I_v^*) = \left(\frac{\pi_h}{\mu_h}, 0, 0, 0, \frac{\pi_v}{\mu_v}, 0 \right). \quad (3. 17)$$

The basic reproduction number (R_{0_b}) for the sub-model (3. 16) is calculated by following the standard next-generation approach [38] and is given by:

$$R_{0_b} = \frac{\sqrt{\mu_h (\alpha \eta + \alpha \mu_h + \alpha \kappa + \mu_h \eta + \mu_h^2 + \mu_h \kappa) \alpha \beta_v \pi_v \beta_h \pi_h}}{\mu_h (\alpha \eta + \alpha \mu_h + \alpha \kappa + \mu_h \eta + \mu_h^2 + \mu_h \kappa) \mu_v}. \quad (3. 18)$$

About the local asymptotic behavior of the sub-model (3. 16), we have the following result: The DFE E_{b0} defined by (3. 17) of the BU only model is locally asymptotically stable if $R_{0b} < 1$.

Proof. To prove the local analysis of the DFE (3. 17), we have to use the linearization approach [39] (Theorem 3.3). For this, we need to calculate the jacobian matrix which is as follows

$$A = \begin{pmatrix} -\mu_h & 0 & 0 & \phi & 0 & -\beta_h \frac{\pi}{\mu_h} \\ 0 & -\alpha - \mu_h & 0 & 0 & 0 & \beta_h \frac{\pi}{\mu_h} \\ 0 & \alpha & -\eta - \mu - \kappa & 0 & 0 & 0 \\ 0 & 0 & \eta & -\phi - \mu_h & 0 & 0 \\ 0 & 0 & -\frac{\pi_v \beta_v}{\mu_v} & 0 & -\mu_v & 0 \\ 0 & 0 & \frac{\pi_v \beta_v}{\mu_v} & 0 & 0 & -\mu_v \end{pmatrix}.$$

The characteristic equation of A is given by

$$\det(A - \lambda I) = 0,$$

or

$$\det \begin{pmatrix} -\mu_h - \lambda & 0 & 0 & \phi & 0 & -\beta_h \frac{\pi}{\mu_h} \\ 0 & -\alpha - \mu_h - \lambda & 0 & 0 & 0 & \beta_h \frac{\pi}{\mu_h} \\ 0 & \alpha & -\eta - \mu - \kappa - \lambda & 0 & 0 & 0 \\ 0 & 0 & \eta & -\phi - \mu_h - \lambda & 0 & 0 \\ 0 & 0 & -\beta_v \frac{\pi_v}{\mu_v} & 0 & -\mu_v - \lambda & 0 \\ 0 & 0 & \beta_v \frac{\pi_v}{\mu_v} & 0 & 0 & -\mu_v - \lambda \end{pmatrix} = 0.$$

By expanding the determinant, we get the following characteristic polynomial:

$$\begin{aligned} & (-\mu_h - \lambda)(-\mu_v - \lambda)(-\phi - \mu_h - \lambda) \left((-\alpha - \mu_h - \lambda)(-\eta - \mu_h - \kappa - \lambda)(-\mu_v - \lambda) \right. \\ & \left. + \frac{\pi_h \beta_h}{\mu_h} \frac{\alpha \pi_v \beta_v}{\mu_v} \right) = 0. \end{aligned} \tag{3. 20}$$

The first three eigenvalues are clearly negative, that is, $\lambda_1 = -\mu_h$, $\lambda_2 = -\mu_v$ and $\lambda_3 = -\phi - \mu_h$. The rest of the eigenvalues can be calculated by simplifying and rearranging the terms as:

$$\begin{aligned} & -\alpha\eta\mu_v - \alpha\mu_h\mu_v - \alpha\kappa\mu_v - \alpha\lambda\mu_v - \mu_h\eta\mu_v - \mu_h^2\mu_v - \mu_h\kappa\mu_v - \mu_h\lambda\mu_v - \lambda\eta\mu_v \\ & -\lambda\mu_h\mu_v - \lambda\kappa\mu_v - \lambda^2\mu_v - \alpha\eta\lambda - \alpha\mu_h\lambda - \alpha\kappa\lambda - \alpha\lambda^2 - \mu_h\eta\lambda - \mu_h^2\lambda \\ & -\mu_h\kappa\lambda - \mu_h\lambda^2 - \lambda^2\eta - \lambda^2\mu_h - \lambda^2\kappa - \lambda^3 + \frac{\alpha\pi_h\beta_h\pi_v\beta_v}{\mu_h\mu_v} = 0, \end{aligned}$$

or

$$\lambda^3 + \lambda^2\Psi_1 + \lambda\Psi_2 + \mu_v(\alpha + \mu_h)(\eta + \mu_h + \kappa)(1 - R_{0b}^2) = 0.$$

For the sake of simplicity, we can write

$$\lambda^3 + \lambda^2\Psi_1 + \lambda\Psi_2 + \Psi_3 = 0. \tag{3. 21}$$

Here

$$\begin{cases} \Psi_1 = \kappa + 2\mu_h + \eta + \alpha + \mu_v, \\ \Psi_2 = \kappa\mu_h + \mu_h^2 + \eta\mu_h + \alpha\mu_h + \alpha\eta + \kappa\mu_v + 2\mu_h\mu_v + \eta\mu_v + \alpha\mu_v, \\ \Psi_3 = \mu_v(\alpha + \mu_h)(\eta + \mu_h + \kappa)(1 - R_{0b}^2). \end{cases} \quad (3. 22)$$

As mentioned above, three of the eigenvalues of the variational matrix are negative and the rest of three can be checked from the roots of equation (3. 21). The coefficient $\Psi_1 > 0$, $\Psi_2 > 0$, and $\Psi_3 > 0$ when $R_{0b} < 1$ (as can be checked from relations (3. 22)). According to Descartes rule of signs, if ψ_1, ψ_2 and ψ_3 are the positive co-efficients of equation (3. 21) then there does not exist any positive real root to the equation. Hence the solutions to the corresponding cubic equation are negative.

Thus, all the eigenvalues of the Jacobean matrix are negative, therefore, the DFE of the BU sub-model (3. 16) is locally asymptotically stable when $R_{0b} < 1$ and unstable otherwise and hence the result. The DFE E_{b0} of the Buruli only model (3. 16) is globally asymptotically stable if $R_{0b} < 1$ and $\Psi = 0$ and unstable otherwise.

Proof. For proving the global stability of the underlying equilibrium point, we consider the Lyapunov function defined by

$$V(t) = a \left(S_h - S_h^* - S_h^* \log \frac{S_h}{S_h^*} \right) + bI_b + cE_b + d \left(S_v - S_v^* - S_v^* \log \frac{S_v}{S_v^*} \right) + eI_v. \quad (3. 23)$$

Differentiating the above function $V(t)$ w.r.t t , we get

$$\begin{aligned} \frac{d}{dt}V(t) &= \frac{d}{dt} \left(a(S_h - S_h^* - S_h^* \log \frac{S_h}{S_h^*}) + bI_b + cE_b + d(S_v - S_v^* - S_v^* \log \frac{S_v}{S_v^*}) + eI_v \right), \\ &= a \left(1 - \frac{S_h^*}{S_h} \right) S_h' + bI_b' + cE_b' + d \left(1 - \frac{S_v^*}{S_v} \right) S_v' + eI_v'. \end{aligned}$$

By using system (3. 16) in the above relation, we have

$$\begin{aligned} V'(t) &= a \left(\frac{S_h - S_h^*}{S_h} \right) (\pi_h + \Phi R_b + -\beta_h I_v S_h - \mu_h S_h) + b(\alpha E_b - (\eta + \mu + \kappa) I_b) \\ &\quad + c(\beta_h I_v S_h - (\alpha + \mu_h) E_b) - \beta_1 E_b + d \left(\frac{S_v - S_v^*}{S_v} \right) (\pi_v - \beta_v I_b S_v - \mu_v S_v) \\ &\quad + e(\beta_v I_b S_v - \mu_v I_v), \\ &= \frac{a}{S_h} (S_h - S_h^*) (\mu_h S_h^* + \Phi R_b - \beta_h I_v S_h - \mu_h S_h) + b(\alpha E_b - (\eta + \mu + \kappa) I_b) + c(\beta_h I_v S_h \\ &\quad - (\alpha + \mu_h) E_b - \beta_1 E_b) + \frac{d}{S_v} (S_v - S_v^*) (\mu_v S_h^* - \beta_v I_b S_v - \mu_v S_v) + e(\beta_v I_b S_v - \mu_v I_v), \\ &= -\frac{a\mu_h}{S_h} (S_h - S_h^*) (S_h - S_h^*) + \frac{a}{S_h} (S_h - S_h^*) (\Phi R_b - \beta_h I_v S_h) + b(\alpha E_b - (\eta + \mu + \kappa) I_b) \\ &\quad + c(\beta_h I_v S_h - (\alpha + \mu_h) E_b - \beta_1 E_b) + \frac{d}{S_v} (S_v - S_v^*) (\mu_v (S_v^* - S_v) - \beta_v I_b S_v) \\ &\quad + e(\beta_v I_b S_v - \mu_v I_v). \end{aligned}$$

By simplification and rearranging the terms, we have

$$\begin{aligned} V(t)' &= -\frac{a}{S_h}\mu_h(S_h - S_h^*)^2 + \frac{a}{S_h}(S_h - S_h^*)(\Phi R_b - \beta_h I_v S_h) + b(\alpha E_b - (\eta + \mu + \kappa)I_b) \\ &\quad + c(\beta_h I_v S_h - (\alpha + \mu_h)E_b - \beta_1 E_b) - \frac{d}{S_v}\mu_v(S_v - S_v^*)^2 - \frac{d}{S_v}(S_v - S_v^*)\beta_v I_b S_v \\ &\quad + e(\beta_v I_b S_v - \mu_v I_v), \\ &= -\frac{a}{S_h}\mu_h(S_h - S_h^*)^2 + \frac{a}{S_h}S_h(\Phi R_b - \beta_h I_v S_h) - \frac{a}{S_h}S_h^*(\Phi R_b - \beta_h I_v S_h) + b(\alpha E_b \\ &\quad - (\eta + \mu + \kappa)I_b) + c(\beta_h I_v S_h - (\alpha + \mu_h)E_b - \beta_1 E_b) - \frac{d}{S_v}\mu_v(S_v - S_v^*)^2 \\ &\quad - \frac{d}{S_v}S_v(\beta_v I_b S_v) + \frac{d}{S_v}S_v^*(\beta_v I_b S_v) + e(\beta_v I_b S_v - \mu_v I_v). \end{aligned}$$

Since, we assumed that $\Phi = 0$, so the above relation becomes

$$\begin{aligned} V(t)' &= -\frac{a}{S_h}\mu_h(S_h - S_h^*)^2 - a\beta_h I_v S_h + \frac{a}{S_h}S_h^*\beta_h I_v S_h + b(\alpha E_b - (\eta + \mu + \kappa)I_b) \\ &\quad + c(\beta_h I_v S_h - (\alpha + \mu_h)E_b - \beta_1 E_b) - \frac{d}{S_v}\mu_v(S_v - S_v^*)^2 - d(\beta_v I_b S_v) \\ &\quad + \frac{d}{S_v}S_v^*(\beta_v I_b S_v) + e(\beta_v I_b S_v - \mu_v I_v). \end{aligned}$$

Upon choosing the constant terms in the above equation as

$$\begin{aligned} a &= c, \quad \frac{a}{\mu_v}S_h^*\beta_h = e, \\ b &= \frac{S_v^*\beta_v}{\eta + \mu_h + \kappa}d, \quad d = \frac{a\beta_h S_h^*}{\mu_h}. \end{aligned}$$

Utilizing these constants and the value of R_{0b} , we get

$$V(t)' = -\mu_h^2\mu_v\frac{(S_h - S_h^*)^2}{S_h} - \mu_v\pi_h\beta_h\frac{(S_v - S_v^*)^2}{S_v} - \mu_h\mu_v(\alpha + \mu_h)(1 - R_{0b}^2)E_b.$$

Here $V(t)' \leq 0$ when $R_{0b} < 1$. Thus, by the LiapunovLasalle theorem [12] (p. 296), the disease free equilibrium E_{b0} of the Buruli ulcer model (3. 16) is globally asymptotically stable under the condition $R_{0b} < 1$ and $\psi = 0$.

3.3. Thy dynamics of the Buruli ulcer and Cholera co-infection model. The disease free equilibrium (E_{0cb}) for model (2. 1) is given by

$$E_{0cb} = (S_h^*, E_b^*, I_b^*, D_{bc}^*, R_b^*, R_c^*, R_{bc}^*, B^*, S_v^*, I_v^*) = \left(\frac{\pi_h}{\mu_h}, 0, 0, 0, 0, 0, 0, 0, \frac{\pi_v}{\mu_v} \right). \tag{3. 25}$$

To calculate the threshold parameter for this model, we shall take the infected classes from model (2. 1) (that is, E_b, I_c, D_{bc}, B, I_v) and will obtain the basic reproduction number (by following [38]) as:

$$R_{0bc} = \max \left\{ \frac{\sqrt{\mu_h(\alpha\eta + \alpha\mu_h + \alpha\kappa + \mu_h\eta + \mu_h^2 + \mu_h\kappa)\alpha\beta_v\pi_v\beta_h\pi_h}}{\mu_h(\alpha\eta + \alpha\mu_h + \alpha\kappa + \mu_h\eta + \mu_h^2 + \mu_h\kappa)\mu_v}, \frac{z\pi_h\omega}{\kappa\mu_h\mu_b(\sigma + \mu_h + \ell)} \right\}.$$

The local analysis of the model is presented in the following theorem. The disease free equilibrium $E_{0_{cb}}$ of the coinfection model (2.1) is locally asymptotically stable if $R_{0_{bc}} < 1$.

Proof. Here again, for proving the local stability of the DFE of the underlying model, we shall utilize the linearization approach. For this, we get the following variational matrix (say \mathcal{K}):

$$\mathcal{K} = \begin{pmatrix} -\mu_h & 0 & 0 & 0 & 0 & \phi & \psi & \theta & -\frac{\pi z}{\kappa \mu_h} & 0 \\ -\beta_h \frac{\pi_h}{\mu_h} & -(\alpha + \mu_h) & 0 & 0 & 0 & 0 & 0 & 0 & 0 & 0 \\ 0 & \alpha & -(\eta + \mu_h + \kappa) & 0 & 0 & 0 & 0 & 0 & 0 & 0 \\ -\beta_h \frac{\pi_h}{\mu_h} & 0 & 0 & -(\sigma + \mu_h + \ell) & 0 & 0 & 0 & 0 & 0 & 0 \\ 0 & 0 & 0 & 0 & -(\delta + \mu_h + \gamma + \varpi) & 0 & 0 & 0 & 0 & 0 \\ 0 & 0 & 0 & 0 & \varepsilon(1 - \delta) & -(\phi + \mu_h) & 0 & 0 & 0 & 0 \\ 0 & 0 & \eta & 0 & (1 - \varepsilon)(1 - \delta) & 0 & -(\psi + \mu_h) & 0 & 0 & 0 \\ 0 & 0 & 0 & \sigma & \delta & 0 & 0 & -(\theta + \mu_h) & 0 & 0 \\ 0 & 0 & 0 & 0 & \omega & \omega \rho & 0 & 0 & 0 & -\mu_b \\ 0 & 0 & 0 & \omega & \omega \rho & 0 & 0 & 0 & 0 & -\mu_b \\ 0 & 0 & -\beta_v \frac{\pi_{uv}}{\mu_v} & 0 & -\beta_v \frac{\pi_{uv}}{\mu_v} & 0 & 0 & 0 & 0 & -\mu_v \\ 0 & 0 & \beta_v \frac{\pi_{uv}}{\mu_v} & 0 & \beta_v \frac{\pi_{uv}}{\mu_v} & 0 & 0 & 0 & 0 & 0 \\ -\mu_v & 0 & 0 & 0 & 0 & 0 & 0 & 0 & 0 & 0 \end{pmatrix}.$$

Next, the characteristic equation is given by $(A - \lambda I) = 0$ and the eigenvalues are obtained by expanding the determinant and it was numerically proved that all of the eigenvalues are negative or complex with negative real parts when $R_{0_{bc}} < 1$. By referring to the approach of [39] (Theorem 3.3), this proves the theorem.

4. OPTIMAL CONTROL THEORY

We utilize the principles of optimal control theory in connection to system (2.1) by incorporating specific controls that can assist in eliminating infection from individuals affected by both cholera and Buruli ulcer. We will apply the Pontryagin's Maximum Principle on the control system in achieving the required conditions. By including the control

variables into the proposed system, we obtain the control system as follows:

$$\left\{ \begin{array}{l} \frac{dS_h}{dt} = \pi_h + \phi R_b + \psi R_c + \theta R_{bc} - (1 - u_1)(\beta_h I_v S_h) - (1 - u_2)\beta_1 S_h - \mu_h S_h, \\ \frac{dE_b}{dt} = (1 - u_1)\beta_h I_v S_h - (\alpha + \mu_h)E_b - \beta_1 E_b, \\ \frac{dI_b}{dt} = \alpha E_b - (1 - u_2)\beta_1 I_b - (u_3\eta + \mu_h + \kappa)I_b, \\ \frac{dI_c}{dt} = (1 - u_2)\beta_1 S_h - (1 - u_1)\beta_h I_v I_c - (u_4\sigma + \mu_h + \ell)I_c, \\ \frac{dD_{bc}}{dt} = (1 - u_1)\beta_h I_v I_c + (1 - u_2)\beta_1 I_b + \beta_1 E_b - (u_5\delta + \mu_h + \gamma + \varpi)D_{bc}, \\ \frac{dR_b}{dt} = u_3\eta I_b - (\phi + \mu_h)R_b + \varepsilon(1 - u_5\delta)D_{bc}, \\ \frac{dR_c}{dt} = u_4\sigma I_c - (\psi + \mu_h)R_c + (1 - \varepsilon)(1 - u_5\delta)D_{bc}, \\ \frac{dR_{bc}}{dt} = u_5\delta D_{bc} - (\theta + \mu_h)R_{bc}, \\ \frac{dB}{dt} = (1 - u_2)\omega(I_c + \rho D_{bc}) - \mu_b B, \\ \frac{dS_v}{dt} = \pi_v - (1 - u_1)\beta_v(I_b + D_{bc})S_v - \mu_v S_v, \\ \frac{dI_v}{dt} = (1 - u_1)\beta_v(I_b + D_{bc})S_v - \mu_v I_v. \end{array} \right. \quad (4. 26)$$

The objective function for the system described in equation (4. 26) is as follows:

$$J(u_i(t)) = \int_0^T (c_1 I_b + c_2 I_c + c_3 D_{bc} + c_4 I_v + c_5 E_b + \sum_{i=1}^5 A_i u_i(t)) dt. \quad (4. 27)$$

Our objective in this control problem is to minimize the Cholera infected, coinfecting, and Buruli ulcer infected individuals, as well as water bugs causing the Buruli ulcer. Additionally, our aim is to minimize the associated expenses related to prevention and treatment measures. The associated control variables with the interpretations are as follows. The controls $u_1(t)$ and $u_2(t)$ describe the actions to stop the spread of both cholera and BU infections. The third control $u_3(t)$ represents the management of individuals with cholera infection and satisfies $0 \leq u_3 \leq g_2$, here g_2 represents the drug's effectiveness in treating individuals infected with cholera. The treatment for individuals infected with BU denoted by $u_4(t)$, designed to manage BU-infected individuals and satisfies $0 \leq u_4 \leq g_3$, where g_3 represents the drug's effectiveness in treating individuals with BU infection. The fifth control $u_5(t)$ is examined here to address the management of both BU and Cholera infected individuals while adhering to the constraint $0 \leq u_5 \leq g_4$, where g_3 represents the drug effectiveness employed for treating individuals infected with cholera and BU. All of the control functions are assumed to be Lebesgue integrable functions and bounded. The final time for the control program is represented by T , and the variables c_i and A_i (where i ranges from 1 to 5) represent the weights and cost factors. Our goal is to find the optimal

control values $u_1^*, u_2^*, u_3^*, u_4^*$, and u_5^* , such that

$$J(u_1^*, u_2^*, u_3^*, u_4^*, u_5^*) = \min_{u_i} J(u_i(t)). \quad (4. 28)$$

The essential requirement that an optimal solution must meet will be derived by using the Pontryagin's Maximum Principle. This principle convert Eqs. (4. 26)-(4. 27) into a type of a problem of minimizing point-wise a Hamiltonian H, with regard to the controls u_1, u_2, u_3, u_4 and u_5 . The Hamiltonian is defined by:

$$\begin{aligned} H = & c_1 E_b + c_2 I_b + c_3 I_c + c_4 D_{bc} + c_5 I_v + A_1 u_1 + A_2 u_2 + A_3 u_3 + A_4 u_4 + A_5 u_5 \\ & + N_{S_h} \{ \pi_h + \phi R_b + \psi R_c + \theta R_{bc} - (1 - u_1)(\beta_h I_v S_h) - (1 - u_2)\beta_1 S_h - \mu_h S_h \} \\ & + N_{E_b} \{ (1 - u_1)\beta_h I_v S_h - (\alpha + \mu_h)E_b - \beta_1 E_b \} \\ & + N_{I_b} \{ \alpha E_b - (1 - u_2)\beta_1 I_b - (u_3 \eta + \mu_h + \kappa)I_b \} \\ & + N_{I_c} \{ (1 - u_2)\beta_1 S_h - (1 - u_1)\beta_h I_v I_c - (u_4 \sigma + \mu_h + \ell)I_c \} \\ & + N_{D_{bc}} \{ (1 - u_1)\beta_h I_v I_c + (1 - u_2)\beta_1 I_b + \beta_1 E_b - (u_5 \delta + \mu_h + \gamma + \varpi)D_{bc} \} \\ & + N_{R_b} \{ u_3 \eta I_b - (\phi + \mu_h)R_b + \varepsilon(1 - u_5 \delta)D_{bc} \} \\ & + N_{R_c} \{ u_4 \sigma I_c - (\psi + \mu_h)R_c + (1 - \varepsilon)(1 - u_5 \delta)D_{bc} \\ & + N_{R_{bc}} \{ u_5 \delta D_{bc} - (\theta + \mu_h)R_{bc} \} \\ & + N_B \{ (1 - u_2)\omega(I_c + \rho D_{bc}) - \mu_b B \} \\ & + N_{S_v} \{ \pi_v - (1 - u_1)\beta_v(I_b + D_{bc})S_v - \mu_v S_v \} \\ & + N_{I_v} \{ (1 - u_1)\beta_v(I_b + D_{bc})S_v - \mu_v I_v \}. \end{aligned} \quad (4. 29)$$

Here the variables $N_{S_h}, N_{E_b}, N_{I_b}, N_{I_c}, N_{D_{bc}}, N_{R_b}, N_{R_c}, N_{R_{bc}}, N_B, N_{S_v}$ and N_{I_v} denotes the associated adjoint variable. The system of adjoint equations can be obtained by applying the appropriate partial differentiations of the Hamiltonian equation (4. 29) with respect to the state variables. The optimal control variables given by $u_1^*, u_2^*, u_3^*, u_4^*, u_5^*$ and the state variables $S_h, I_b, I_c, I_c, D_{bc}, R_b, R_c, R_{bc}, B, S_v$, and I_v minimizing $J(u_1, u_2, u_3, u_4, u_5)$ over the admissible control set, the adjoint variables given by $N_{S_h}, N_{E_b}, N_{I_b}, N_{I_c}, N_{D_{bc}}, N_{R_b}, N_{R_c}, N_{R_{bc}}, N_B, N_{S_v}$ and N_{I_v} satisfies

$$-\frac{dN_i}{dt} = \frac{\partial H}{\partial i}, \text{ where } i \text{ stand for the state variable,}$$

with the transversality conditions

$$\begin{cases} N_{S_h}(T) = N_{E_b}(T) = N_{I_b}(T) = N_{I_c}(T) = N_{D_{bc}}(T) = N_B(T) = 0, \\ N_{R_b}(T) = N_{R_c}(T) = N_{R_{bc}}(T) = N_{S_v}(T) = N_{I_v}(T) = 0, \end{cases} \quad (4. 30)$$

and the characterization of the optimal control are given by

$$\begin{aligned}
u_1^* &= \min \left\{ 1, \max \left(0, \frac{\beta_h I_v S_h (N_{E_b} - N_{S_h}) + \beta_h I_v I_c (N_{D_{bc}} - N_{I_c}) + \beta_v S_v (I_b + D_{bc}) (N_{I_v} - N_{S_v})}{A_1} \right) \right\}, \\
u_2^* &= \min \left\{ 1, \max \left(0, \frac{\frac{BzS_h(N_{I_c} - N_{S_h})}{\kappa + B} + \frac{BzI_b(N_{D_{bc}} - N_{I_b})}{\kappa + B} + \omega(I_c + \rho D_{bc})N_B}{A_2} \right) \right\}, \\
u_3^* &= \min \left\{ 1, \max \left(0, \frac{\eta I_b (N_{I_b} - N_{R_b})}{A_3} \right) \right\}, \\
u_4^* &= \min \left\{ 1, \max \left(0, \frac{\eta I_c (N_{I_c} - N_{R_c})}{A_4} \right) \right\}, \\
u_5^* &= \min \left\{ 1, \max \left(0, \frac{\delta D_{bc} (N_{D_{bc}} + N_{R_{bc}}) + \varepsilon \delta D_{bc} N_{bc} N_{R_b} - (1 - \varepsilon) \delta D_{bc} N_{R_c}}{A_5} \right) \right\}.
\end{aligned} \tag{4.31}$$

Proof. By employing the Pontryagin's Maximum Principle to the Hamiltonian equation and relevant state variables of the control system in conjunction with the optimality system, we can derive the set of adjoint equations. Upon calculation and reorganization, we arrive

at the adjoint system as follows:

$$\begin{aligned}
\frac{dN_{S_h}}{dt} &= (1 - u_1)\beta_h I_v(N_{S_h} - N_{E_b}) + (1 - u_2)\frac{Bz}{\kappa + B}(N_{S_h} - N_{I_c}), \\
\frac{dN_{E_b}}{dt} &= -c_1 + (\alpha + \mu_h + \frac{Bz}{\kappa + B})N_{E_b} - N_{I_b}\alpha - \frac{Bz}{\kappa + B}N_{D_{bc}}, \\
\frac{dN_{I_b}}{dt} &= -c_2 + (1 - u_2)\frac{Bz}{\kappa + B}(N_{I_b} - N_{D_{bc}}) - u_3\eta N_{R_b} + (1 - u_1)\beta_v S_v(N_{S_v} - N_{I_v}) \\
&\quad + (u_3\eta + \mu_h + \kappa)N_{I_b}, \\
\frac{dN_{I_c}}{dt} &= -c_3 + (1 - u_1)\beta_h I_v(N_{I_c} - N_{D_{bc}}) - u_4\sigma N_{R_c} + (u_4\sigma + \mu_h + \ell)N_{I_c} - \omega(1 - u_2)N_B, \\
\frac{dN_{D_{bc}}}{dt} &= -c_4 + (u_5\delta + \mu_h + \gamma + \varpi)D_{bc} - \varepsilon(1 - u_5\delta)N_{R_b} - (1 - \varepsilon)(1 - u_5\delta)N_{R_c} - u_5\delta N_{R_{bc}} \\
&\quad - (1 - u_2)\omega\rho N_B + (1 - u_1)\beta_v S_v(N_{S_v} - N_{I_v}), \tag{4.32} \\
\frac{dN_{R_b}}{dt} &= (\phi + \mu_h)N_{R_b} - \phi N_{S_h}, \\
\frac{dN_{R_c}}{dt} &= (\phi + \mu_h)N_{R_c} - \psi N_{S_h}, \\
\frac{dN_{R_{bc}}}{dt} &= (\phi + \mu_h)N_{R_{bc}} - \theta N_{S_h}, \\
\frac{dN_B}{dt} &= (1 - u_2)S_h \frac{\kappa z}{(\kappa + B)^2}(N_{S_h} - N_{I_c}) + (1 - u_2)I_b \frac{\kappa z}{(\kappa + B)^2}(N_{I_b} - N_{D_{bc}}) \\
&\quad + \frac{\kappa z}{(\kappa + B)^2}E_b(N_{E_b} - N_{D_{bc}}) + \mu_b N_B, \\
\frac{dN_{S_v}}{dt} &= (1 - u_1)\beta_v(I_b + D_{bc})(N_{S_v} - N_{I_v}) + \mu_v N_{S_v}, \\
\frac{dN_{I_v}}{dt} &= -c_5 + (1 - u_1)\beta_h S_h(N_{S_h} - N_{E_b}) + (1 - u_1)\beta_h I_c(N_{I_c} - N_{D_{bc}}) + \mu_v N_{I_v}.
\end{aligned}$$

Next, by applying the condition $\frac{\partial H}{\partial u_i} = 0$, we have the desired characterization of the control variables (4.31). In the next part, we will present numerical solution of the model that will validate the analytical results obtained thus far and will support the obtained optimum model. Further, we shall derive strategies that help in minimizing the severity of the diseases within the population.

5. NUMERICAL SIMULATION

In this section, we will simulate the behavior of the proposed mathematical model that will explain and predict the behavior of the underlying dynamical systems. For simulating the proposed model, we use fourth order Runge- Kutta (RK4) method to get the numerical solution of the model and of the optimal control system. It is the most commonly used method to find the solution of differential equation. Algorithm of the RK4 method for a first order differential equation $y' = f(x, y)$, $y(x_0) = y_0$ is given below:

$$y_n = y_{n-1} + \frac{1}{6}(k_1 + 2k_2 + 2k_3 + k_4),$$

where

$$\begin{aligned}
 k_1 &= hf(x_{n-1}, y_{n-1}), \\
 k_2 &= hf\left(x_{n-1} + \frac{1}{2}h, y_{n-1} + \frac{1}{2}k_1\right), \\
 k_3 &= hf\left(x_{n-1} + \frac{1}{2}h, y_{n-1} + \frac{1}{2}k_2\right), \\
 k_4 &= hf(x_{n-1} + h, y_{n-1} + k_3).
 \end{aligned}$$

We use the above algorithm of RK4 and simulated the model by considering different values of the parameters in subsequent examples.

Example 5.1 (Numerical simulation of model (3. 2) for $(R_0 < 1)$).

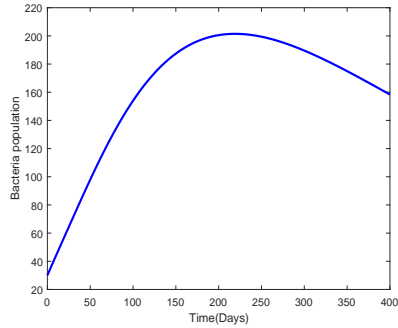
According to Theorems (3.1) and (3.1) , if $(R_0 < 1)$, then the model will be locally as well as globally asymptotically stable, which means that the disease will be eliminated from the population. As a result, we have chosen the following initial condition:

$$((S_h(1), I_c(1), R_c(1), B(10)) = (100, 30, 100, 30))$$

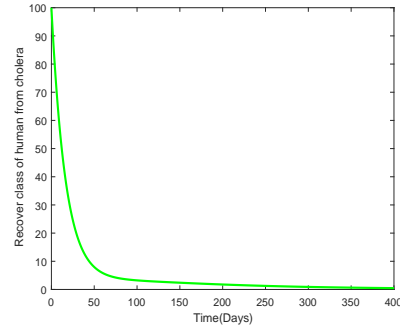
. Other values of the parameters are given in Table (2). Using these values, the graphical representation of the proposed model compartmental-wise is given in Figure 1.

Parameter	Value	Parameter	Value
π_h	0.25 2	ψ	0.055
μ_h	0.005	σ	0.006
μ_b	0.0035	ω	0.051
ℓ	0.009	β_1	0.005
z	0.0001111	κ	0.007

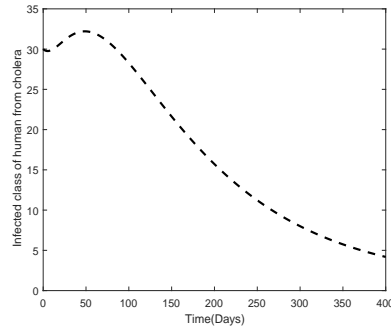
TABLE 2. Parameter and their numerical value used in the numerical simulation of sub-model (3. 16)



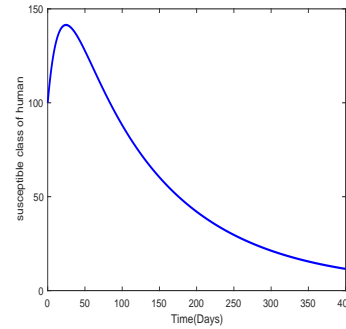
(A) The plot shows the time-evolution of the bacteria population.



(B) The plot describes the dynamics of the human recovered from the Cholera.



(C) The progression of the Cholera' infected population with time.



(D) The plot shows the dynamics of the human population vulnerable to Cholera infection.

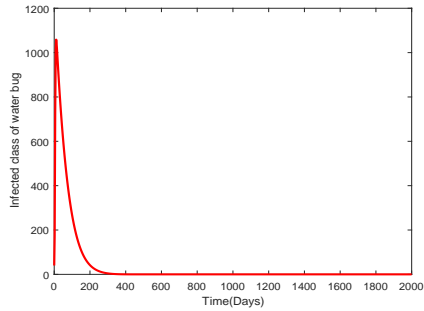
FIGURE 1. The time-evolution of the bacteria causing Cholera and the population of human being recovered, infected and vulnerable to the Cholera infection for $R_{0_c} < 1$.

Example 5.2 (Simulations of model (3. 16) for $R_0 < 1$).

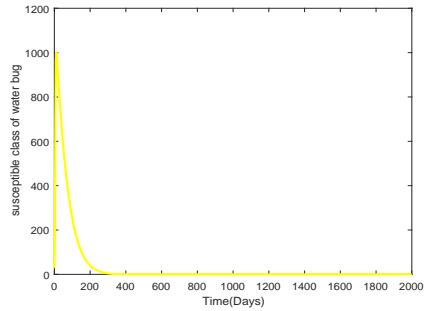
According to Theorems (3.2) and (3.2) , if $R_0 < 1$, then the model will be locally as well as globally asymptotically stable, which means that the disease will be eliminated from the population. As a result, we can choose the following values of the parameters in below Table with initial condition:

$$(S_h(1), E_b(1), I_b(1), R_b(1), S_v(1), I_v(1)) = (100, 100, 30, 100, 30, 40).$$

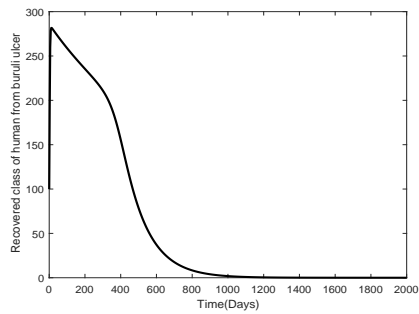
Using these values, the graphical representation of the proposed model compartmental-wise are given in Figure 2.



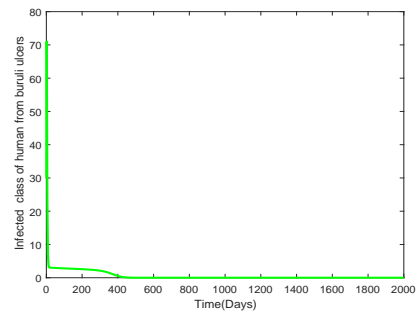
(A) The plot shows the dynamics of the infected water bug.



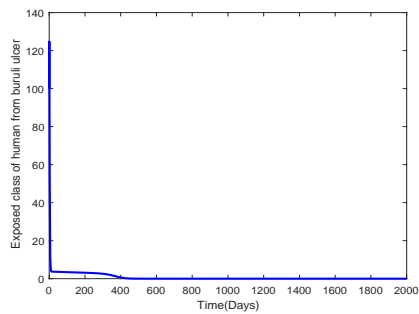
(B) The time-evolution of the susceptible water bug.



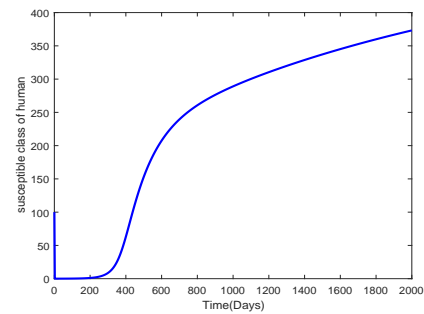
(C) The graph shows the human population recovered from the Buruli ulcer.



(D) The people infected from the Buruli ulcer and its dynamical behavior.



(E) Dynamical behavior of the individual exposed to Buruli ulcer.



(F) People vulnerable to Buruli ulcer and its evolution with time.

FIGURE 2. Numerical Simulation of model (3. 16) subject to $R_{0b} = 0.0043 < 1$

Parameter	value	Parameter	value
π_h	0.25	α	0.55
μ_h	0.0005	η	0.6
π_v	0.95	μ_v	0.0519
β_1	0.05	β_h	0.04
β_v	0.013	ϕ	0.007
κ	0.07		

TABLE 3. Parameter and their numerical value used in the numerical simulation of sub-model (3. 16)

Example 5.3 (Numerical solution of the model (2. 1) for $R_0 < 1$).

According to Theorem (3.3) , if $R_0 < 1$, then the model will be locally asymptotically stable, which means that the disease will be eliminated from the population. As a result, we can choose the following values of the parameters given in Table (4) with the initial condition:

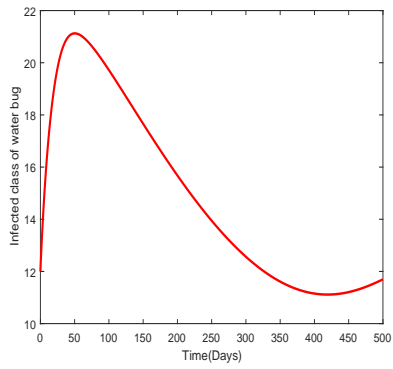
$$(S_h(1), E_b(1), I_b(1), I_c(1), D_{bc}(1), R_b(1), R_c(1), R_{bc}(1), B(1), S_v(1), I_v(1)) \quad (5. 33)$$

$$= (100, 10, 20, 20, 15, 12, 14, 13, 12, 13, 12). \quad (5. 34)$$

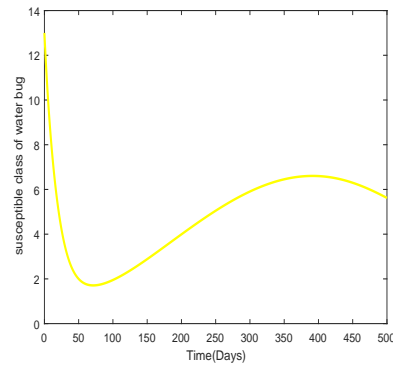
Using these values, the graphical representation of the proposed model compartmental-wise is given below.

Parameter	Value	Parameter	Value
π_h	0.00025	π_v	0.0095
ϕ	0.007	ψ	0.005
θ	0.06	μ_h	0.05
μ_b	0.051	β_h	0.004
β_v	0.0015	κ	0.004
φ	0.0005	γ	0.0009
ℓ	0.0005	ε	0.0001
δ	0.00001	η	0.00001
ρ	0.0007	β_1	0.005
α	0.006	σ	0.0002
ω	0.0070	μ_v	0.0051
φ	0.007		

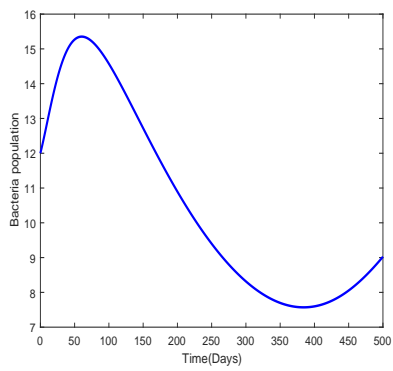
TABLE 4. Parameter and their numerical value used in the numerical simulation of model (2. 1)



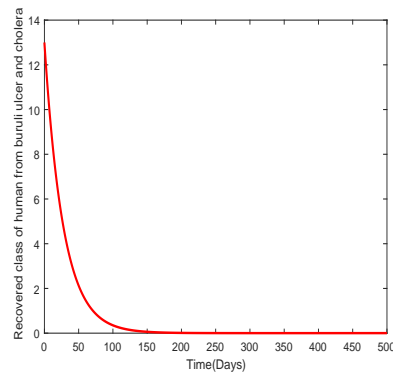
(A) The plot shows the co-dynamics of the infected water bug.



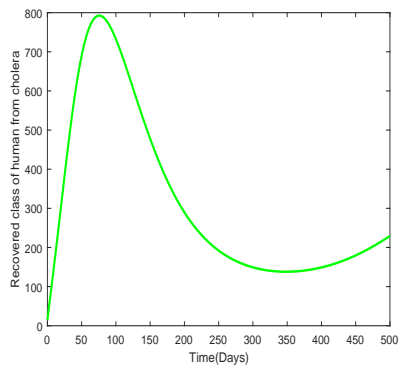
(B) The co-time-evolution of the susceptible water bug.



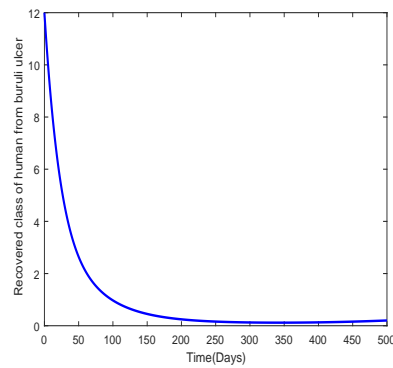
(C) The dynamics of the bacteria populations when both the diseases persist.



(D) Recovered people both from the Buruli ulcer and Cholera.

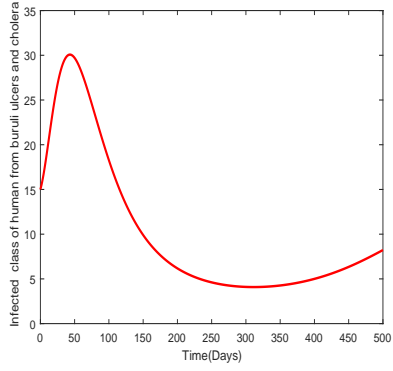


(E) The dynamics of the human population getting recovery from the Cholera.

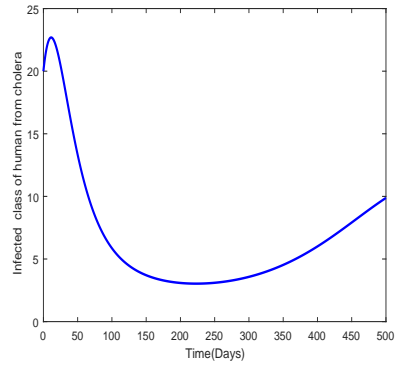


(F) The co-dynamics of the human population getting recovery from the Buruli ulcer.

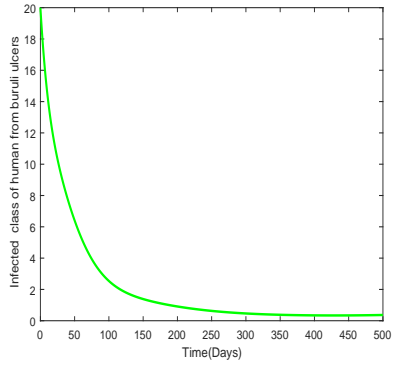
FIGURE 3. Numerical Simulation of model (2. 1) subject to $R_{0bc} = 0.2458 < 1$.



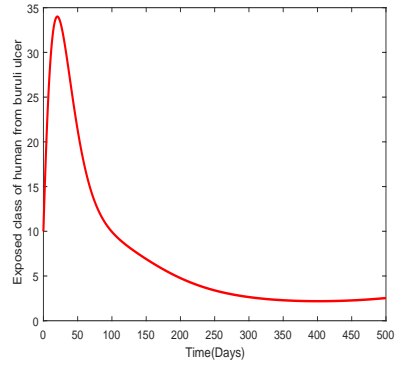
(A) The plot represent the co-dynamic of the human population infected from Cholera and Buruli ulcer both.



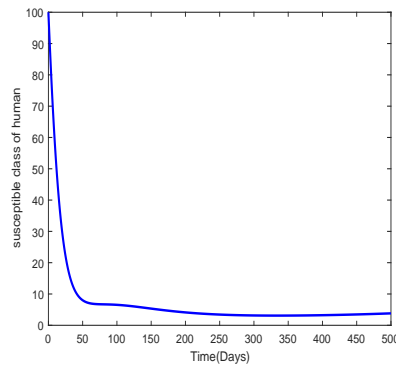
(B) The dynamic of the Cholera infected people.



(C) The dynamics of the individuals infected from the Buruli ulcer only.



(D) The co-dynamics of the individuals exposed to Buruli ulcer only.



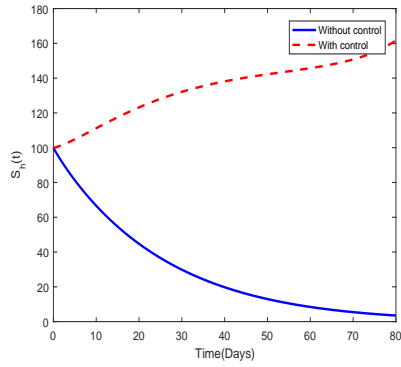
(E) The plot shows the co-time-evolution of the human population vulnerable to either Buruli ulcer or Cholera.

FIGURE 4. The plot shows numerical solution of the state variables involve in model (2. 1) subject to $R_{0bc} = 0.2458 < 1$.

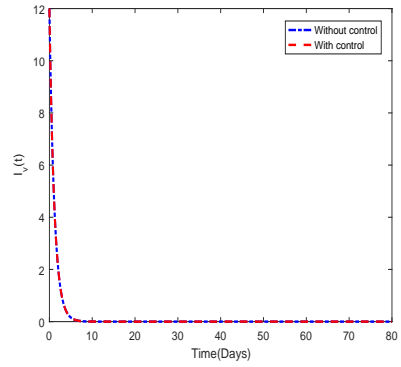
5.4. Numerical simulation on the optimal control problem. In this example, we numerically solve the optimality system (4.26) and the proposed model without control by using the RK4 method and assess several control strategies based on their sensitivity to the system. The initial values of the control are calculated and the optimality condition is changed for subsequent iterations by solving the state system forward through time and the adjoint system backward in time. Our aim is to minimize the number of infected individuals with either BU or Cholera or both and also to minimize the relative cost with the prevention program. The sample solutions of both models are plotted in the subsequent figures.

We can see from figure 5a, without the control variable the populations of susceptible people decreases with time but when we apply the control variable then the populations of susceptible people increases with time. One can notice from Figure 5b, the control variable effect on infected water bug is negligible i.e without the control variable and with control variable the population of the infected water bug is almost same. We see from figure 5c that the control variable effect on susceptible water bug is negligible i.e without the control variable and with control variable the population of the susceptible water bug is almost same. It can be observed from Figure 5d that without the control variable the population of bacteria populations increases with time but when we apply the control then the bacteria populations decreases with time. Figure 5e suggest that the control variable effect on recovers people from both bururli ulcer and cholera is negligible i.e without the control variable and with control variable the population of the recovers people from both bururli ulcer and cholera almost same. We see that from the above figure 5f, without the control variable the populations of recover peoples from cholera increases with time but when we apply the control variable then the populations of recover peoples from cholera slightly more increases with time.

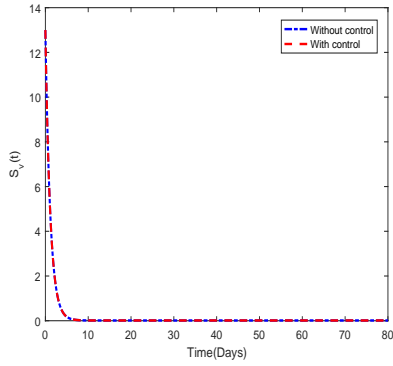
We see that from the above figure 6a, without the control variable the populations of recover peoples from Buruli ulcer decreases with time but when we apply the control variable then the populations of recover peoples from Buruli ulcer slightly less decreases with time. we see that from the above figure 6b, without the control variable the populations of infected peoples from both Buruli ulcer and cholera decreases with time but when we apply the control variable then the populations of infected peoples from both Buruli ulcer and cholera slightly more decreases with time. We see that from the above figure 6c, without the control variable the populations of infected peoples from cholera increases with time but when we apply the control variable then the populations of infected peoples from cholera decreases and approach to zero with time. We see that from the above figure 6d, without the control variable the populations of infected peoples from Buruli ulcer decreases with time but when we apply the control variable then the populations of infected peoples from Buruli ulcer slightly more decreases with time.



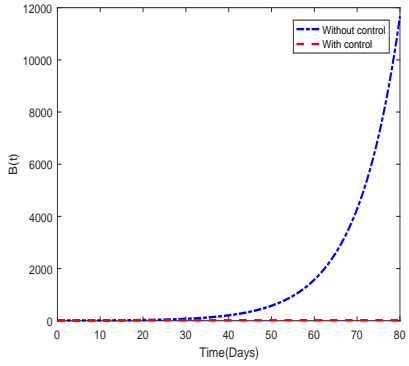
(A) The control and without control plots of the human susceptible to either Buruli ulcer or Cholera.



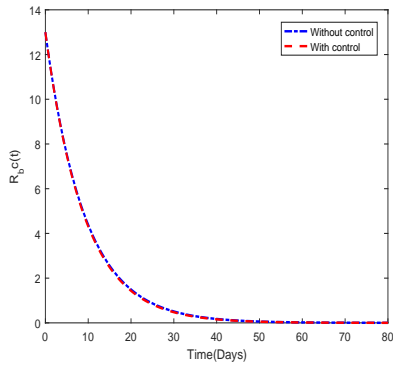
(B) The time-evolution of the infected water bug both in the presence and absence of the control variables.



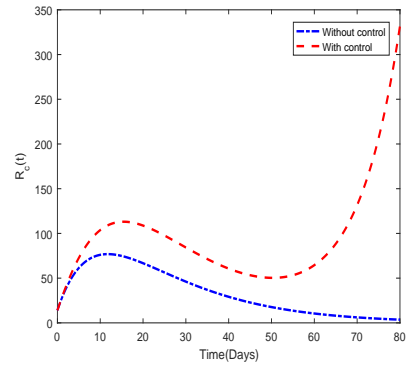
(C) The co-dynamics of the susceptible water bug both in the presence and absence of the control variables.



(D) The population of the bacteria in the presence and absence of the control measures.

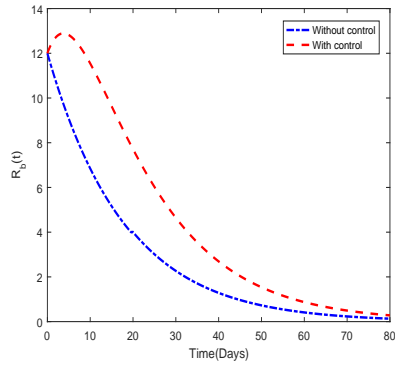


(E) The co-dynamics of the recovered human from both the diseases and in the presence and absence of the control variables.

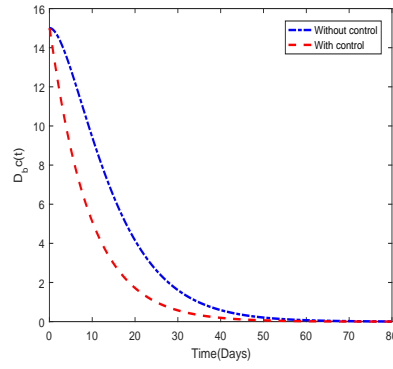


(F) The population of the Cholera' recovered individuals both with and without control measures.

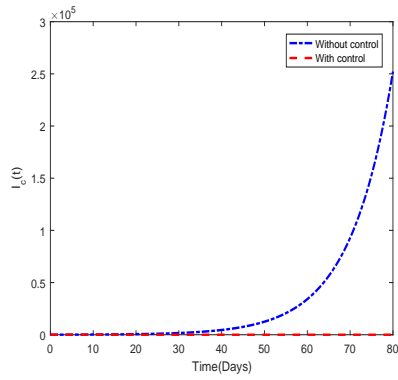
FIGURE 5. The plot shows the dynamic behavior of the solution components of the control and without control models for a given set of parameter values.



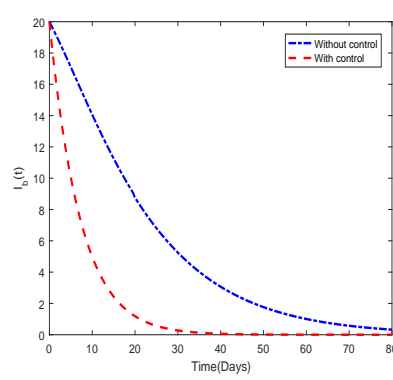
(A) The dynamics of the people getting recovery from the Buruli ulcer both with and without control variables.



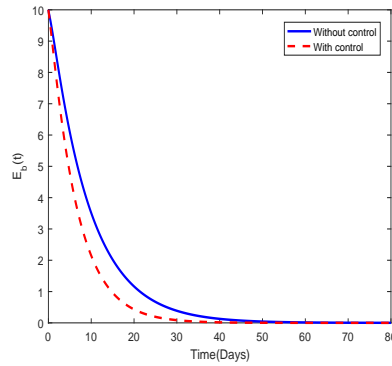
(B) The control and without control co-dynamics of the infected human from both the disease.



(C) The dynamics of the people infected with Cholera both with and without control variables.



(D) The control and without control plots of the human infected with the Buruli ulcer.



(E) The control and without control plots of the human exposed to Buruli ulcer.

FIGURE 6. Numerical solution of various components of the control and without control models for a given set of parameter values.

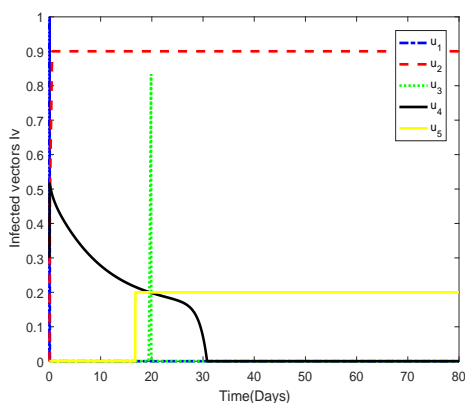


FIGURE 7. The time evolution of the control variables.

In the graph 7, we have plotted the control variables and its dynamics were shown as the time evolves. Some of the control variables attain the maximum and minimum while others are changing with time.

6. CONCLUSION

In our current study, we thoroughly investigated the co-dynamics of cholera and Buruli ulcer by employing the tools of mathematical modeling. We effectively modeled and analyzed the Cholera and Buruli ulcer infections, individually and when they occur together, via evolutionary differential equations. We investigated the sub-models related to Cholera and Buruli ulcer, and obtained the mathematical results about the persistence and extinction of the infections. We analyzed the local and global behaviors of the sub-models when the value of R_0 is less than 1. We found that these sub-models exhibit stability at fixed points both locally and globally under certain conditions. Furthermore, we explored the model for the co-infection and discuss its stability in the local sense when R_0 is less than 1. We formulate optimal control problems, considering five different control variables to manage Cholera and Buruli ulcer infections, and their co-infections. We provided a detailed necessary conditions about the optimum system. To verify analytical results and to see the effectiveness of the control variables, we performed numerical simulations, considering various combinations of parameters.

In the future research work, the authors intend to extend the idea of co-infection of these two disease into fractional modeling by following the concepts of [3]. The authors have also a keen interest in the modeling of the novel growing research area of diabetes and glucose-insulin interaction models keeping in view the base studies like [1, 29]. Further, the researcher can conduct similar co-dynamic studies for different infectious diseases using age-structured models.

FUNDING

This work is partly supported by the *Undergraduate Research Support Program* under the project for building the provincial STI system of the *Directorate General of Science and Technology (DoST)*, Government of Khyber Pakhtunkhwa awarded vide letter no. DGST/BPSTI/UGRS/2022-23-8794 dated April 5, 2023.

CONFLICT OF INTEREST

The authors declare that they have no competing interests.

AUTHOR'S CONTRIBUTION STATEMENT

Asaf Khan: Methodology, Conceptualization, Supervision **Gauhar Ali:** Formal Analysis, Writing - original draft, Methodology, **Abdul Khaliq:** Formal Analysis, Writing - original draft, Methodology **Gul Zaman:** Conceptualization, Writing - review editing, Validation.

REFERENCES

- [1] K.I. Ahmed, H.D. Adam, M.Y. Youssif and S. Saber. *Different strategies for diabetes by mathematical modeling: Applications of fractalfractional derivatives in the sense of AtanganaBaleanu*. Results in Physics **52**, (2023): 106892.
- [2] A.Y. Aidoo and B. Osei. *Prevalence of aquatic insects and arsenic(as) concentration determine the geographical distribution of Mycobacterium ulcerans infection*. Comput Math Methods Med **8**, (2007):235244.
- [3] N. Almutairi, S. Saber, and H. Ahmad. *The fractal-fractional Atangana-Baleanu operator for pneumonia disease: stability, statistical and numerical analyses*. AIMS Mathematics **8**, No. 12 (2023): 29382-29410.
- [4] R.M. Anderson and R.M. May. *Infectious Diseases of Humans: Dynamics and Control*. Oxford: Oxford University Press, 1991.
- [5] M. Bachar, J. Batzel, and S. Ditlevsen. *Stochastic Biomathematical Models with Applications to Neuronal Modeling*, Springer **41**, (2012): 3.
- [6] D. Bernoulli. *Essai d'une nouvelle analyse de la mortalit cause per la petite vroleet les avantages de linoculation pour la prvenir Histoire de l'Academie Royale des Sciences*. Anne, 1760.
- [7] J.G. Boyles, P.M. Cryan, G.F. McCracken, T.H. Kunz. *Economic importance of bats in agriculture*. Science, **332**(2011):412.
- [8] F.E-G Cox. *History of the discovery of the malaria parasites and their vectors*. Department of Infectious and Tropical Diseases, London School of Hygiene and Tropical Medicine, London, WCIE 7HT, UK 2010.
- [9] K. Diez and J. Heesterbeek. *Bernoullis epidemiological model revisited*. Math. Biosci. **180**, (2002): 121.
- [10] A.S. Fauci and D.M. Morens. *Zika Virus in the Americas Yet another arbovirus threat*. N Engl J Med **374**, (2016):601-4.
- [11] *Global Health Observatory Data Repository*. [Accessed: 28 June 2022]. Available: <http://apps.who.int/gho/data/node.main.A1631>.
- [12] J.K. Hale. *Ordinary Differential Equations*. Wiley-Interscience, New York, 1969.
- [13] D.M. Hartley, Jr. J.G. Morris, D.L. Smith. *Hyper-infectivity: A critical element in the ability of V. cholerae to cause epidemics?*. PLoS Medicine **3**, (2006): 00630069.
- [14] H.W. Hethcote. *The mathematics of infectious diseases*. SIAM Review **42**, (2000): 599–653.
- [15] T. Junghanss, R.C. Johnson, G. Pluschke. *Mycobacterium ulcerans disease*. Manson tropical infectious diseases. Twenty-Third. London: W.B. Saunders; 2014, 519531.e2.
- [16] W. Kermack and A. Mckendrick. *A contribution to mathematical theory of epidemics*. Proc. Roy. Soc. Lond. A. **115**, (1927): 700-721.
- [17] S. Knobler, A. Mahmoud, S. Lemon, and L. Pray. *The impact of globalization on infectious disease emergence and control, Exploring the consequences and opportunities*, institute of medicine (US) forum on microbial threats, Washington (DC): National Academies Press (US); 2006.

- [18] B.W. Lerner and K.L. Lerner. *Infectious Diseases: Exceptionally fine Authoritative Comprehensive*. American Library Association. Choice, **2**, 2008.
- [19] S. Levin, *A thousand and one epidemic models*, in *In Frontiers in Mathematical Biology*, vol. 100 of Lecture Notes in Biomathematics, Springer, Berlin, 1994, 504515.
- [20] *Middle East respiratory syndrome coronavirus (MERS-CoV) Republic of Korea*, <http://www.who.int/westernpacific/emergencies/2015-mers-outbreak> Accessed: 12 March, 2024.
- [21] F. Nadeem, M. Hikmat, M. Zamir and W.K. Mashwani. Threshold Condition for Elimination of Zoonotic Visceral Leishmaniasis. Punjab Univ. J. Math **56**, No. 6 (2024).
- [22] F. Nadeem, M. Zamir, A. Tridane and Y. Khan. Modeling and control of zoonotic cutaneous leishmaniasis. Punjab Univ. J. Math **51**, No. 2, (2019): 105121.
- [23] R.L.M. Neilan, E. Schaefer, H. Gaff, K.R. Fister, S. Lenhart. *Modeling optimal intervention strategies for cholera*. Bull Math Biol **72**, (2010): 20042018.
- [24] K.S. Nisar, M. Farman, M. Abdel-Aty and J. Cao. *Mathematical epidemiology: A review of the singular and non-singular Kernels and their applications*. Progr. Fract. Differ. Appl **9**, No. 4 (2023):507-544.
- [25] D. Ofori-Adjei and K. Koram. *Editorial commentary on Cholera and Ebola virus disease in Ghana*. Ghana Med J. **48**, No. 3(2014):120.
- [26] K.O. Okosun, O.D. Makinde. *A co-infection model of malaria and cholera diseases with optimal control*. Math Biosci **258**, (2014):1932.
- [27] C.I. Piccolo and L. Billings. *The effect of vaccinations in an immigrant model*. Math. Comput. Model. **42**, (2005): 291299.
- [28] P. Roumagnac, F.X. Weill, C. Dolecek, S. Baker, S. Brisse, N.T. Chinh, T.A.H. Le, C.J. Acosta, J. Farrar, G. Dougan and M. Achtman. *Evolutionary history of salmonella typhi*. Science **314**, (2006): 1301-1304.
- [29] S. Saber, A. Alalyani. *Stability analysis and numerical simulations of IVGTT glucose-insulin interaction models with two time delays*. Mathematical Modelling and Analysis, **27**, No. 3 (2022):383-407.
- [30] M. U. Saleem, M. Farman, K. S. Nisar, A. Ahmad Z. Munir and E. Hincal. *Investigation and application of a classical piecewise hybrid with a fractional derivative for the epidemic model: Dynamical transmission and modeling*. Plos one **19**, No. 8 (2024):e0307732.
- [31] M.D.L. Sen and S. Alonso-Quesada. *Vaccination strategies based on feedback control techniques for a general SEIR epidemic model*. Applied Mathematics and Computation **218**, No. 7 (2011): 38883904.
- [32] M.D.L. Sen, R.P. Agarwal, A. Ibeas and S. Alonso-Quesada. *On a generalized time-varying SEIR epidemic model with mixed point and distributed time-varying delays and combined regular and impulsive vaccination controls*. Advances in Difference Equations **2010**, (2010):Article ID 281612.
- [33] B. Shulgin, L. Stone and Z. Agur. *Pulse vaccination strategy in the SIR epidemic model*. Bull. Math. Biol. **60**, (1998): 1123-1148.
- [34] M.T. Sofonea. *Epidemic models: why and how to use them*. PMC - NCBI.
- [35] M.F. Tabassum, M. Farman, A. Akgil and S. Akram. *Mathematical treatment of nonlinear pine wilt disease model: An evolutionary approach*. Punjab Univ. J. Math **54**, No. 9, (2022): 607620.
- [36] D. Thompson, P. Muriel, D. Russell, P. Osborne, A. Bromley, M. Rowland, et al. *Economic costs of the foot and mouth disease outbreak in the United Kingdom in 2001*, Rev. Sci. Tech. Int. des. Epizoot. **21**(2002):67585.
- [37] E. Tognotti, *The dawn of medical microbiology: Germ hunters and the discovery of the cause of cholera*. History of Medicine and Human Sciences, Medical School, Department of Biomedical Sciences, Italy 2011.
- [38] P. Van den Driessche, and J. Watmough. *Reproduction numbers and sub-threshold endemic equilibria for compartmental models of disease transmission*. Mathematical Biosciences **180**, No. 1-2 (2002):29-48.
- [39] G. De Vries, T. Hillen, M. Lewis, J. Miller and B. Schnfisch. *A course in mathematical biology: quantitative modeling with mathematical and computational methods*. Society for Industrial and Applied Mathematics, 2006.
- [40] WHO, *Swine influenza in humans*, http://www.who.int/influenza/human_animal_interface/en, Accessed 12 March 2024.
- [41] WHO, Available:http://apps.who.int/iris/bitstream/10665/77771/1/9789241503402_eng.pdf
- [42] WHO. *Cholera vaccines: WHO position paper*. Weekly epidemiological record **85**, (2010): 117–28.
- [43] S. Yadav and G. Rawal. *The current mental health status of Ebola survivors in Western Africa*. J Clin Diagn Res. **9**, No. 10 (2015):LA01-LA02.

- [44] S. Yadav, G. Rawal. *Swine flu: Have we learnt any lessons from the past?*. Pan Afr Med J. **22** (2015):118.
Zhao
- [45] J.Q. Zhao, E. Bonyah, B. Yan, M.A. Khan, K.O. Okosun, M.Y. Alshahrani and T. Muhammad. *A mathematical model for the coinfection of buruli ulcer and cholera*. Results in Physics **29**, (2021): 104746.